

ФИЗИКА ПРОЧНОСТИ И ПЛАСТИЧНОСТИ

PACS numbers: 52.77.Fv, 61.66.Dk, 62.20.M-, 62.20.Qp, 81.20.Vj

The Influence of Hydrogen Addition to Argon as a Shielding Gas on the Fatigue Performance of TIG Welded AISI 304 Stainless Steel

E. Gözütok and N. Kahraman

*Karabuk University,
Technology Faculty,
78050 Karabuk, Turkey*

In this study, AISI 304 austenitic stainless steel sheets are joined through TIG welding under various shielding media. Bending fatigue, notch impact and bending tests are performed on the joined materials. Hardness of the joined materials is also determined. The welding processes are carried using pure argon, argon + 1.5% H₂ and argon + 5% H₂ as shielding media at three different welding currents. Both butt and overlap welding processes are carried out at the same welding parameters. The ER 308 L type wire is used as the filler material for all the joints. The highest fatigue and impact strengths are obtained for both types of joints for argon shielding media. The bending test is applied up to 180°, and no tearing, crack or any other bending defects after visual examination of the bended samples are observed. The welding metal gives the highest hardness values, and they are followed by HAZ and base material.

У даному дослідженні листи неіржавійної аустенітної сталі AISI 304 з'єднувалися газовольфрамовим дуговим зварюванням у середовищі різних захисних газів. З'єднані матеріали були піддані тестам на вигин, утомним випробуванням на вигин та випробуванням на ударний вигин із розрізом. Визначалася також твердість з'єднаних матеріалів. Процеси зварювання виконувалися з використанням чистого аргону, аргону + 1,5% H₂ та аргону + 5% H₂ як захисних середовищ при трьох різних струмах зварювання. Виконувалося як зварювання зі стиком упритул, так і внаслідок при однакових параметрах зварювання. Для всіх зварювальних швів як присаджувальний матеріал використовувався дріт типу ER 308 L. Для обох типів швів найбільша утомна і ударна міцність були одержані при використанні аргонового захисного середовища. Випробування на вигин виконувалися до значень кута вигину у 180°; при цьому на зігнутих зразках візуально не спостерігалося жодних розривів, тріщин та будь-яких інших дефектів вигину. Зварюваний метал мав найвищу твердість як у пришовній зоні, так і в основному матеріалі.

В данном исследовании листы нержавеющей austenитной стали AISI 304 соединялись газовольфрамовой дуговой сваркой в среде различных защитных газов. Соединённые материалы были подвергнуты тестам на изгиб, усталостным испытаниям на изгиб и испытаниям на ударный изгиб с разрезом. Определялась также твёрдость соединённых материалов. Процессы сварки производились с использованием чистого аргона, аргона + 1,5% H₂ и аргона + 5% H₂ в качестве защитных сред при трёх разных токах сварки. Выполнялась как сварка встык, так и внахлест при одинаковых параметрах сварки. Для всех сварных швов в качестве присадочного материала использовалась проволока типа ER 308 L. Для обоих типов швов наибольшая усталостная и ударная прочности были получены при использовании аргоновой защитной среды. Испытания на изгиб проводились до значений угла изгиба в 180°; при этом на согнутых образцах визуально не наблюдалось никаких разрывов, трещин и любых других дефектов изгиба. Свариваемый металл обладал наивысшей твёрдостью как в окколошовной зоне, так и в основном материале.

Key words: TIG welding, hydrogen, mixture gas, fatigue, mechanical properties.

(Received November 22, 2011)

1. INTRODUCTION

Stainless steel can be a confusing material to those unfamiliar with the alloys as the term stainless steels refers to a large family of material types and alloys [1]. The physical characteristics of stainless steel, including high strength and ductility, weldability [2], durability, ease of forming and machining, good fire resistance, and ready re-use and recycling make this material ideally suited [3] and relatively new material for use in construction [4]. Stainless steel or, more precisely, corrosion-resisting steels are a family of iron-base alloys having excellent resistance to corrosion due to the passive films on the surface [5–7]. These properties make austenitic stainless steels attractive candidate materials for use in the fabrication of kitchen goods, piping systems [2], and in a variety of equipment associated with the chemical and nuclear power industries [2, 8].

Austenitic stainless steel is one of the most important categories of stainless steels, accounting for nearly 70% of the total amount of stainless steels that have been produced [9]. Austenitic stainless steels are widely used in food processing, pulp and paper, chemical, petrochemical and nuclear industries mainly because they have excellent corrosion resistance [10]. Among them, type 304 stainless-steel sheets are most commonly used for forming products since they are superior in formability [6, 11] and have adequate weldability [12]. However, it is structurally metastable and undergoes a partial phase transformation when subjected to sufficient stress or strain [13]. Gas tungsten arc welding (GTAW) is one of the commonly used welding methods for

stainless steel [14]. GTAW is suitable for welding thin materials when good quality and surface finish are required [15].

Argon (Ar) gas is the most commonly used shielding gas for GTAW for stainless steel. Helium (He) gas causes a high heat input due to high arc energy and thermal conductivity, and thus supports increasing welding speed and weld penetration [16]. Hydrogen has been added to argon in welding of stainless steels only recently [6, 14, 17]. The addition of hydrogen to argon permits increased welding speeds [6, 18]. Hydrogen also significantly increases the volume of molten material in the weld pool due to the higher thermal conductivity of argon-hydrogen mixtures at temperatures at which molecules of hydrogen dissociate [6, 14].

In the present work, AISI 304 austenitic stainless steel sheets are welded by TIG welding method, under various shielding media and at various current values. Bending fatigue, notch impact, bending performances and hardness of the joined materials are investigated.

2. EXPERIMENTAL PROCEDURES

Austenitic stainless steel (X5CrNi1810) with the dimensions of $400 \times 80 \times 1.5$ mm³ and with the quality AISI 304 is used for this experimental work. Schaeffler diagram is used in order to anticipate the microstructure in advance that can be formed during joining. As can be seen from Fig. 1, the main material is shown as A while the additional

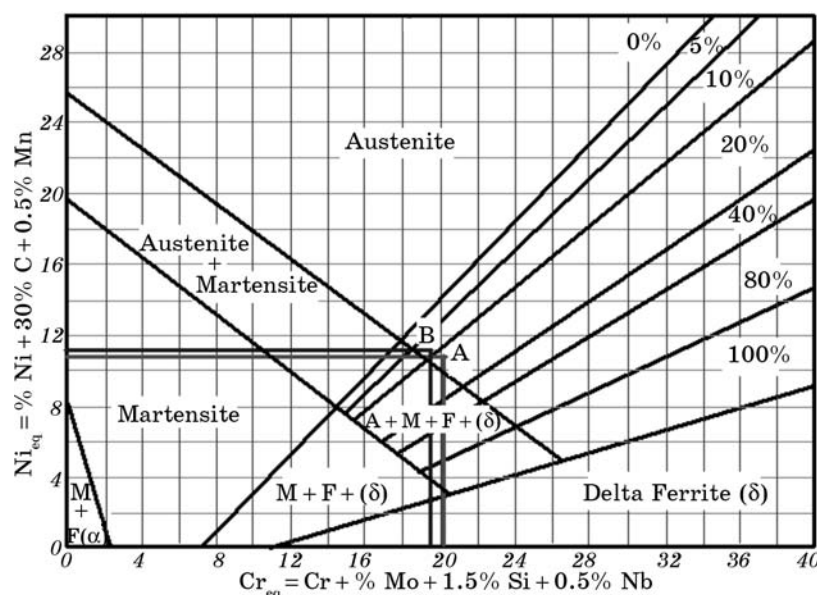


Fig. 1. Schaeffler diagram.

material is shown as B on the diagram by calculating the equivalences of chrome and nickel of the main and additional metals. In accordance with the diagram, it is assumed that welding compositions may contain 10% delta ferrite phase in austenitic matrix. The chemical composition (% vol.) and the calculated Cr_{eq} and Ni_{eq} equivalence values of the base metal used are given in Table 1. Moreover, ER 308 L wire 2 mm in diameter is used during welding process as filler material and the chemical composition of this material, and its Cr_{eq} and Ni_{eq} values are shown in Table 2.

Welding processes were carried out using a CEBORA AC-DC 2030-M model inverter type welding machine having a tungsten electrode of 2.4 mm in diameter under three different shielding gas atmospheres. Welding parameters used during experiments are shown in Table 3. At each parameter, butt and overlap welding methods are performed. The overlap distance is chosen as 10 mm and the welding is carried out at the both sides. Six welding operations were carried out.

The starting and end points of the welded parts are cut off at 20 mm away through water jet and fatigue, notch impact, bending and hardness tests samples are prepared from the remaining parts as shown in Fig. 2. Whereas the samples for fatigue are prepared from samples of both butt and overlap welded joints, the samples for notch impact, bending and hardness examinations are prepared only from butt-welded joint.

For hardness measurements, butt welded samples are first cold

TABLE 1. Chemical combination of main material.

Element	Chemical composition								Equivalence value	
	C	Cr	Si	Mn	Ni	Mo	Nb	Fe	Cr_{eq}	Ni_{eq}
Weight, %	0.042	18.45	0.75	1.50	8.56	0.48	0.021	Balance	20.06	10.57

TABLE 2. Chemical composition of additional material.

Element	C	Si	Mn	Cr	Ni	Fe	Cr_{eq}	Ni_{eq}
Weight, %	<0.02	0.5	1.7	20.1	9.8	Balance	19.68	11.25

TABLE 3. The used welding parameters.

Shielding media	Current, A	Gas stream ratio, min ⁻¹	Welding speed, cm/min
Argon	80	12	12
Argon + 1.5% H ₂	70	12	12
Argon + 5% H ₂	60	12	12

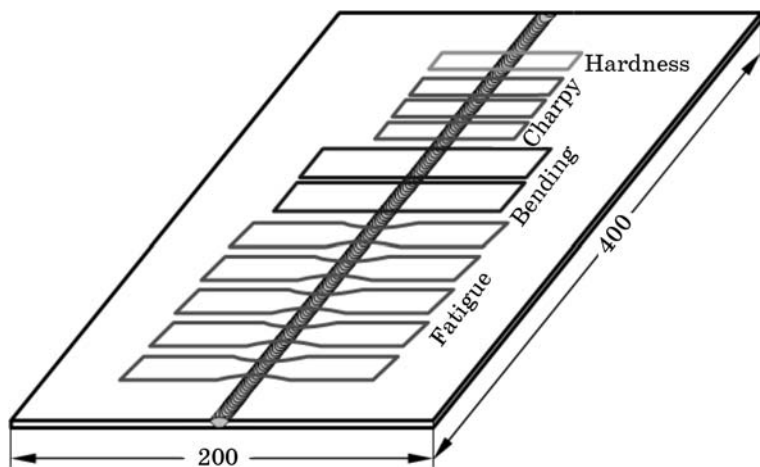


Fig. 2. Schematic illustration of characterization samples.

mounted in bakelite and then standard metallographic procedures (grinding, polishing and etching) are applied. *HV* hardness measurements of the welded samples are performed using a Shimadzu HMV hardness measuring unit. In hardness measurements, a load of 500 g is used and the averages of 5 measurements results for each part are calculated.

Eight samples for fatigue tests were prepared for each gas mixture through water jet cutting in standard dimensions (EN 288-3). The dimensions of butt and overlap welded fatigue samples are given in Fig. 3. Schematic illustration of the fatigue testing unit on which the

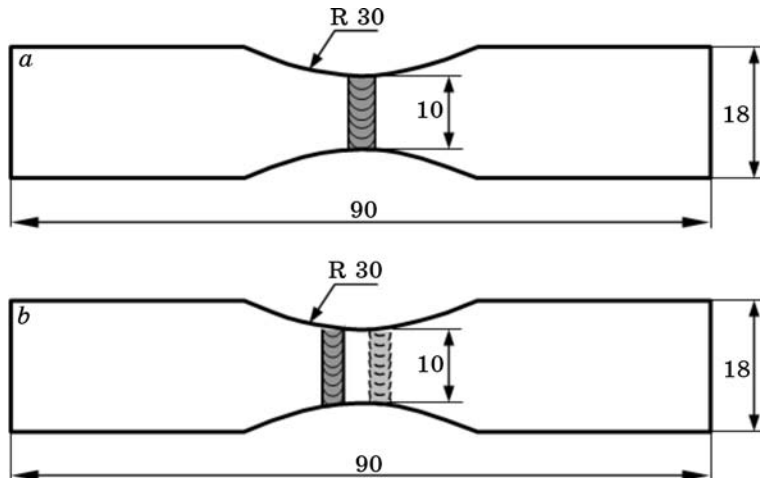


Fig. 3. Dimensions of fatigue samples: butt-welded (a) and overlap-welded (b).

butt and overlap welded joints were subjected to fatigue tests is shown in Fig. 4.

Bending fatigue test results and Wöhler curves were constructed logarithmically against the maximum number of cycle corresponding to the highest stress. Eight samples from the welded joints were prepared. In addition, one sample from the base material was prepared for comparison purpose. Boundary cycle number N is determined to be $2 \cdot 10^6$ for all the tests based on the previous studies. Bending stress σ values are calculated using the bending momentum M_e used in the tests for rectangular cross-section through classical strength calculations as follows [19]:

$$W = bh^3/12, \quad \sigma = M_e/W,$$

where σ —bending stress (kg/cm^2), W —axial resistance momentum (cm^3), M_e —bending momentum ($\text{kg}\cdot\text{cm}$), b —width (cm), h —thickness (cm).

The bending fatigue testing unit is stopped automatically with a magnetic stop mechanism that stops the circuit when the sample is broken or fractured during the tests. The counter mounted to the motor shaft shows the total bending cycle until fracture. A total of 12 notch impact samples were prepared as 3 samples from each weld metal and main material. The dimensions of the notch impact samples are shown in Fig. 5.

Thicknesses of the welded samples were reduced to the thickness of

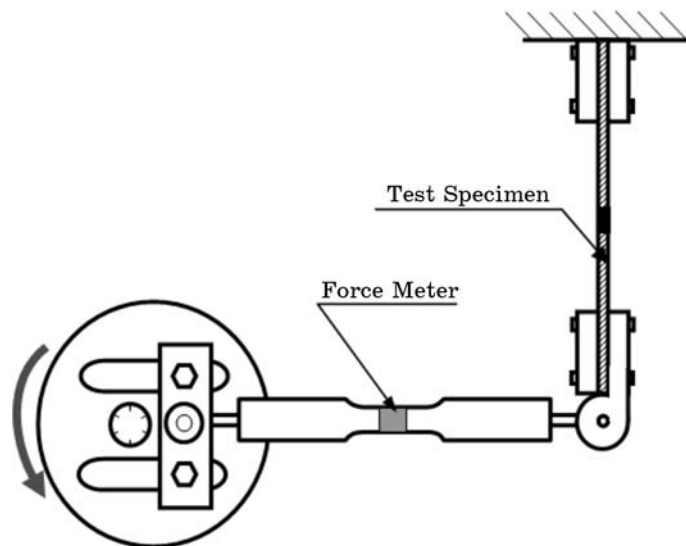


Fig. 4. Schematic illustration of the fatigue testing unit.

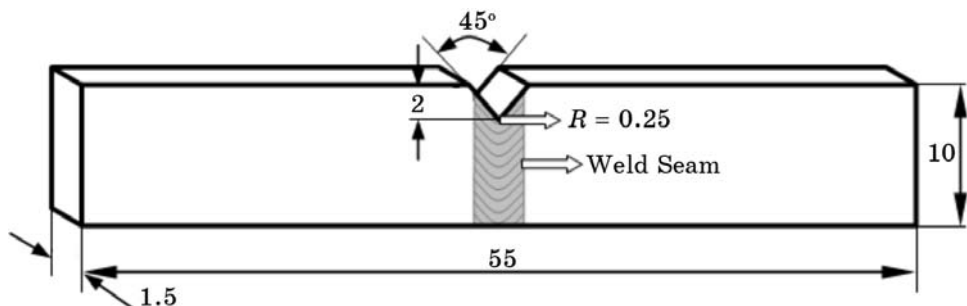


Fig. 5. Notch impact test sample.

base material by machining. The notches of the samples are formed on a milling machine and then the samples are subjected to impact test on Devotrans Devo (CDC 0700014) impact unit at room temperature.

The bending test samples were prepared according to EN 910 with the dimensions of $20 \times 160 \text{ mm}^2$ from only the butt welded joints through water jet cutting. The weld roots and depths of the water jet cut samples were reduced to the base material thickness through grinding. Two pieces of bending test samples were prepared from each welded joints. Three point bending tests were carried out using Autograph-Shimadzu tensile-compression unit at 2 mm/min bending speed.

3. RESULTS AND DISCUSSIONS

3.1. Hardness Test

The hardness test gives an idea of the wear resistance of the weld metal. Hardness values can give information about the metallurgical changes caused by welding. When the hardness test results in Fig. 6 are evaluated, it is seen that there is a decrease in hardness from welding zone to base metal. Heat affected zone (HAZ) and base metal follow it while the maximum hardness values belong to welding material. In a similar study, Tusek *et al.* [20] join austenitic stainless steel sheets with MIG welding method and it is demonstrated that hardness values decrease as the distance from the welding material increases.

When the joints obtained under different shielding media are compared, it is seen that although there is not a significant difference, the highest level of hardness is obtained with Argon + 5% H₂ and this is followed by with Argon + 1.5% H₂. The lowest hardness value is measured for the joints welded under pure argon atmosphere. In a similar study, Abuç [21] joins AISI 304 austenitic stainless steels under various shielding media using 308 L welding wire and determines their hardness values. The highest hardness value is obtained at the weld

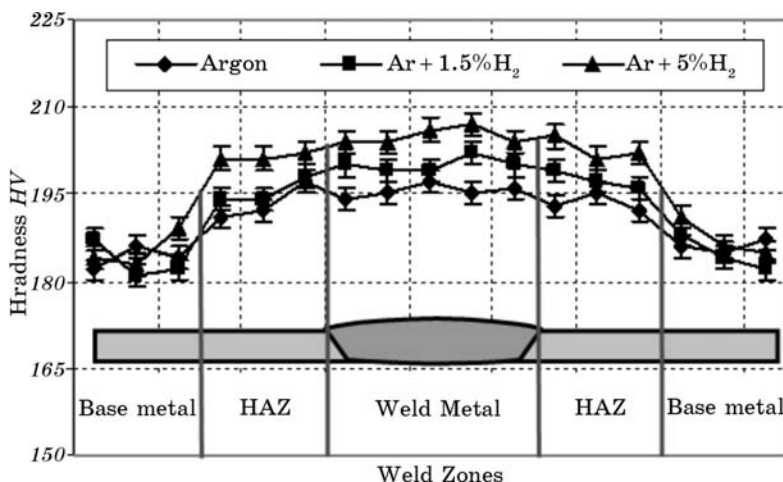


Fig. 6. Hardness measurement results.

metal. Moreover, he suggests that the joints produced under argon gas have lower hardness values than those joined under Argon + 5% H₂ protective gas.

3.2. Bending Fatigue Test

Bending fatigue behaviour of three butt-welded joints produced under pure argon, argon + 1.5% H₂ and argon + 5% H₂ and base material are wholly shown in Fig. 7. When we examine the curves, it is seen that the welded samples have lower bending fatigue lives than that of base material. This was attributed to the heat input to the welding zone, which leads to structural deteriorations. Yuri *et al.* [22] and Sivaprasad and Raman [23] investigated the bending fatigue properties of welded materials and reported that bending fatigue resistances of main materials are higher than those for welded materials. Moreover, when the fractured surfaces of welded materials are examined, it is seen that fracture mostly takes place at HAZ, which is the weakest point of joints. Similar findings were also observed in another study, which is about bending fatigue lives of friction stir welded aluminium alloy materials [19].

As seen from Fig. 7, the highest bending fatigue strength takes place in the base material. Whereas the highest bending fatigue strength for the welded materials is demonstrated in the samples joined under argon gas and this is followed by argon + 1.5% H₂ and argon + 5% H₂. When the welded samples joined under H₂ containing shielding media are examined, the more H₂ added, the lower the bending fatigue strength and the more possibility to fracture is seen.

When the bending fatigue resistances of base material and overlap

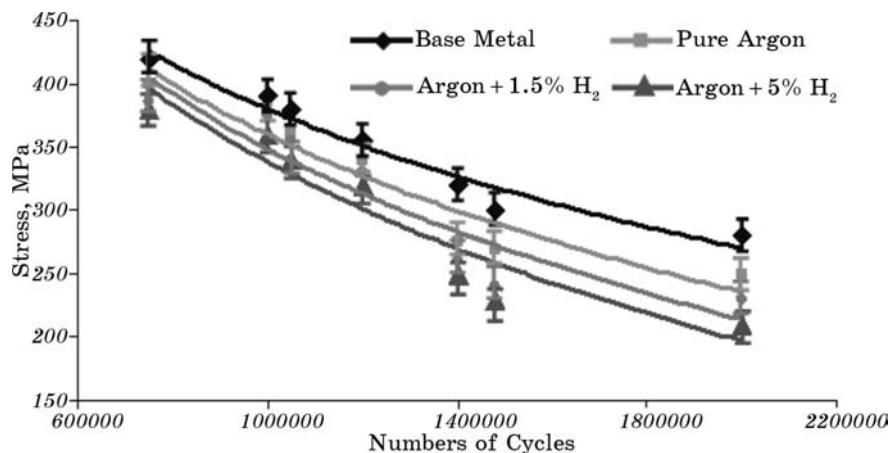


Fig. 7. Bending fatigue resistances of base material and butt-welded samples joined under three different shielding gas compositions.

welded samples joined under three different shielding gas compositions (pure argon, argon + 1.5% H₂ and argon + 5% H₂) are compared, the bending fatigue strength of the base metal is seen to be higher than those of the overlap welded joints. The bending fatigue strength of the overlap-welded sample joined under pure argon is seen to be higher than the others joined under H₂ added shielding media.

For both the butt welded (Fig. 7) and overlap welded (Fig. 8) joints, it is observed that increasing hydrogen addition to argon gas as shielding media decreased the bending fatigue strengths of the welded joints. The larger hydrogen addition corresponds to the lower bending

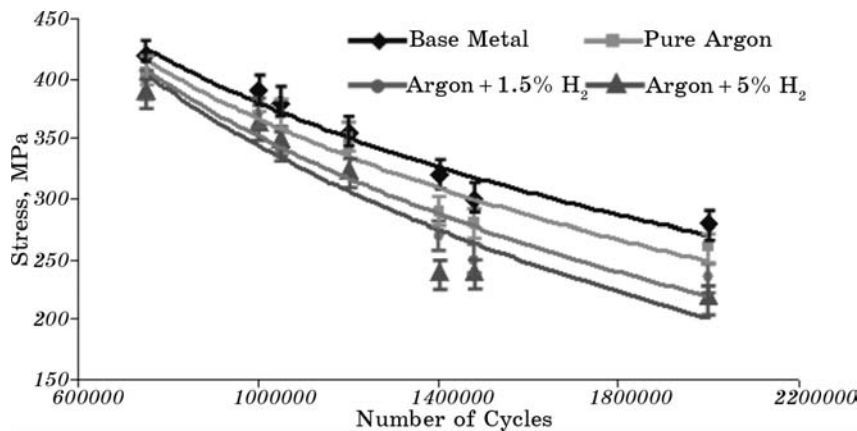


Fig. 8. Bending fatigue resistances of base material and overlap welded samples joined under three different shielding gas compositions.

fatigue strength. This is attributed to the presence of hydrogen in molecular form in the welding zone and its contribution to crack growth. During welding H₂ is dissociated and brought into the welding zone in atomic form. Within the material, it recombines and diffuses to eventually forms voids within the material that initiate cracks. Tusek and Suban [17] state that hydrogen addition to shielding gas in TIG welding causes some problems like bubbles and cracks.

In welded austenitic stainless steels, diffusion of hydrogen in weld metal to HAZ and grain growth at high welding temperatures are critical regarding the quality of weldability. This affects the fatigue life of welded parts. Molecular hydrogen breaks down to atomic form at the high arc plasma temperatures within the welding arc. Hydrogen ions are then absorbed into the molten weld pool and transported through the weld metal and into the parent metal HAZ by diffusion. This diffusion stage is particularly important where the weldment experiences a longer cooling phase, causing austenitic grain growth in the HAZ during the austenitization stage. It appears that weld metal hydrogen content rises at the fusion line and gradually decreases further away throughout the parent metal HAZ. The hydrogen content of the HAZ rises because of hydrogen diffusion into the parent metal [24].

Some hydrogen in shielding gas is entrapped into weld metal and HAZ after cooling and this, in turn, leads to cracks especially in transition zone over time. The diffused hydrogen gathers at the three axes stress zone (at sharp corners of dislocations and microcracks). This increases stress crack propagation. Therefore, increasing hydrogen addition to shielding gas decreases bending fatigue resistance.

It is reported in another study [25] that the ingress of hydrogen into metals can occur in several ways depending on material type, the presence of hydrogen in the form of atomic hydrogen, and factors such as the solubility of atomic hydrogen, the pressure of hydrogen, and stress. The first route involves separating reservoir fluids into oil, gas, and formation water. The second route is associated with the introduction of hydrogen into the weld pool during welding.

When the bending fatigue strengths of the butt and overlap welded joints are compared, it is seen that the overlap-welded joints are better than the butt-welded joints; see Figs. 7 and 8. It is thought that the reason for this might be the overlap weld geometry that increases the strength.

3.3. Impact Test

Impact test is employed to check the ability of a weld to absorb energy under impact without fracturing. This is a dynamic test, in which a single blow breaks a test specimen, and the energy used in breaking the piece is measured in foot-pounds. This test compares the toughness of

the weld metal and HAZ with the base metal. It is useful in finding if the welding process destroyed any of the mechanical properties of the base metal.

The notch impact test results of the base material and butt-welded joints are presented in Fig. 9. The notch impact tests are carried out only in order to compare the base metal and welded samples and the welded samples among themselves (in order to see the effects of H_2 gas addition to argon).

When Figure 9 is examined, it is seen that the highest notch impact resistance belongs to base material with 18.1 J. The highest notch impact resistance among the weld metals of three different samples joined under three different shielding gases belongs to the sample with 17.9 J joined under pure argon shielding gas. That sample is followed by argon + 1.5% H_2 with 17.5 J and argon + 5% H_2 with 16.4 J. It can be concluded from this result that H_2 gas added to argon shielding gas decreases the notch impact resistance. When argon + H_2 gas is used, the heat input to welding zone is increased and δ -ferrite amount in the welding zone is also increased. Increasing δ -ferrite amount in the weld metal having body centred cubic structure leads to decreasing notch impact resistance values. Liao and Chen [26] also stated that δ -ferrite has influence on the notch toughness of all the weld metals.

When notch impact test results are examined, it is seen that weld metals of the welded samples are not as tough as the base material. Moreover, the shielding gases used during welding affect the weld metal toughness value. If the notch impact values of weld metals of the welded samples shown in Fig. 9 and hardness values given in Fig. 6 are compared, it is seen that when hardness values measured at welding metals are increased, toughness decreases. At a similar study on weld metals of different metals, Kılınçer and Kahraman [27] reported that

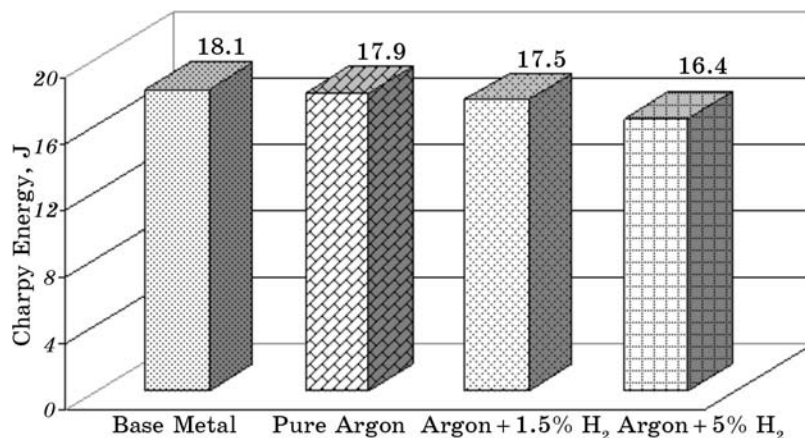


Fig. 9. Notch impact test results of base material and butt-welded samples.

notch impact resistance is decreased in accordance with the increase of hardness of weld metal.

3.4. Bending Test

The quality of the weld metal at the face and root of the welded joint, as well as the degree of penetration and fusion to the base metal, are determined by means of guided bend tests. To fulfil the requirements of this test, the specimens must be bent 180° and, to be acceptable, no cracks greater than 1/8 in. (3.2 mm) in any dimension should appear on the surface.

The bending photos of the butt-welded samples joined under three different shielding gases (pure argon, argon + 1.5% H₂ and argon + 5% H₂) are given in Fig. 10. During the bending tests, a careful visual examination was made in order to determine the crack-starting angle of the welded samples and it was seen that all of the samples were bended up to 180° without any problem. No cracks, tears, etc. are seen by visual quality control of the bended samples.

After recognizing that there are no cracks at the weld zones (weld metal, HAZ and base material) of the bended samples, it is seen that the welded joints are in accordance with the standards and the welded joints can be easily bended and used in service conditions. Moreover, the bending of welded joints up to 180° without any fracture shows that the welding is sound. In their similar studies, Gülenç *et al.* [6] and Durgutlu [14] joined austenitic stainless steels under pure argon and argon with various amounts of hydrogen additions and reported that there are no cracks and tears after 180° bending tests.

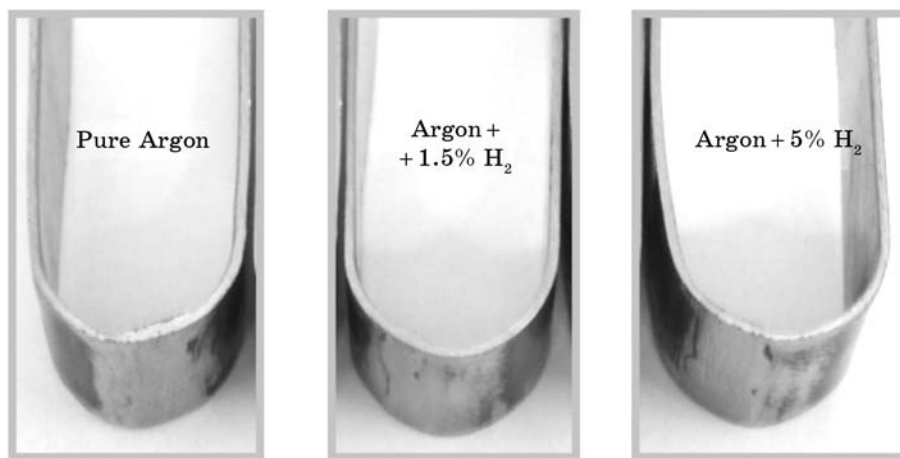


Fig. 10. After bending photos of butt-welded joints.

4. CONCLUSIONS

The following conclusions can be drawn from this study:

1. According to hardness test results, at all the shielding media, the highest strength value is measured from the weld metal and this is followed by HAZ and base material.
2. According to bending fatigue test results, the bending fatigue values of the both butt and overlap welded joints are found to be lower than those for the base material.
3. It is seen that the increasing H_2 gas addition to argon gas reduced the bending fatigue strength of the welded joints.
4. When the butt and overlap welded joints are compared among themselves, it is seen that the fatigue strength of the overlap welded joints is found to be slightly better than those for the butt welded joints.
5. According to the notch impact test results, the toughness values of all the welded joints were lower than those for the base material. Moreover, the H_2 gas added to argon decreased the notch impact values slightly.
6. According to the bending test results, the specimen bended up to 180° showed no traces of crack and tear.
7. Although, the H_2 addition deteriorates some properties of the welded joints, it might be advantageous for some applications as less energy is required. Besides, hydrogen addition to the argon as shielding gas increases melting efficiency of TIG welding of austenitic stainless steel.

REFERENCES

1. G. Gedge, *J. Constr. Steel Res.*, **64**: 1194 (2008).
2. F. Karci, R. Kaçar, and S. Gündüz, *J. Mater. Process Tech.*, **209**: 4011 (2009).
3. M. Ashraf, L. Gardner, and D. A. Nethercot, *J. Constr. Steel Res.*, **62**: 105 (2006).
4. G. Kiymaz, *Thin Wall Structures*, **43**: 1534 (2005).
5. H. Takuda, K. Mori, T. Masachika, E. Yamazaki, and Y. Watanabe, *J. Mater Processing Tech.*, **143–144**: 242 (2003).
6. B. Gülenç, K. Develi, N. Kahraman, and A. Durgutlu, *Int. J. Hydrogen Energy*, **30**: 1475 (2005).
7. X. Gao, J. Tang, Y. Zuo, Y. Tang, and J. Xiong, *Corros. Sci.*, **51**: 1822 (2009).
8. L. W. Tsay, S. C. Yu, and R. T. Huang, *Corros. Sci.*, **49**: 2973 (2007).
9. Z. Z. Yuan, Q. X. Dai, Q. Zhang, X. N. Cheng, and K. M. Chen, *Mater. Charact.*, **59**: 18 (2008).
10. H. Dong, P. Y. Qi, X. Y. Li, and R. J. Llewellyn, *Mat. Sci. Eng. A*, **431**: 137 (2006).
11. H. B. Carry, *Modern Welding Technology*. 2nd Ed. (New Jersey: American Welding Society: 1981), p. 497.
12. H. U. Hong, B. S. Rho, and S. W. Nam, *Int. J. Fatigue*, **24**: 1063 (2002).

13. M. Topic, R. B. Tait, and C. Allen, *Int. J. Fatigue*, **29**: 656 (2007).
14. A. Durgutlu, *Mater. Design*, **25**: 19 (2004).
15. H. Y. Huang, *Mater. Design*, **30**: 2404 (2009).
16. B. Y. Kang, Y. K. D. V. Prasad, M. J. Kang, H. J. Kim, and I. S. Kim, *J. Mater. Processing Tech.*, **209**: 4722 (2009).
17. J. Tusek and M. Suban, *Int. J. Hydrogen Energy*, **25**: 369 (2000).
18. A. D. Althouse, C. H. Turnquist, W. A. Bowditch, and K. E. Bowditch, *Modern Welding* (IL, South Holland: Goodheart-Wilcox Company Inc.: 1992), p. 327.
19. M. K. Külekci and A. Şık, *Arch. Metall. Mater.*, **51**: 213 (2006).
20. J. Tusek, Z. Kampus, and M. Suban, *J. Mater. Processing Tech.*, **119**: 180 (2001).
21. S. Abuç, *The Effect of Shielding Gas Composition on Mechanical Properties of Austenitic Stainless Steels Welded by GTAW* (MSc Thesis) (Sakarya: Sakarya University: 2006), p. 23.
22. T. Yuri, T. Ogata, M. Saito, and Y. Hirayama, *Cryogenics*, **40**: 251 (2000).
23. S. Sivaprasad and G. S. Raman, *Mater. Sci. Eng. A*, **448**: 120 (2007).
24. M. Pitrun, *The Effect of Welding Parameters on Levels of Diffusible Hydrogen in Weld Metal Deposited using Gas Shielded Rutile Flux Cored Wires* (PhD Thesis) (Wollongong: The University of Wollongong: 2004), p. 27.
25. J. R. Still, *Welding Journal*, **83**: 26 (2004).
26. M. T. Liao and W. J. Chen, *Mater. Chem. Phys.*, **55**: 145 (1998).
27. S. Kılınçer and N. Kahraman, *J. Fac. Eng. Archit. Gazi Univ.*, **24**: 23 (2009).